Published in final edited form as:
Cancer Res. 2010 March 15; 70(6): . doi:10.1158/0008-5472.CAN-09-2503.

Preclinical evaluation of radiation and perifosine in a genetically and histologically accurate model of brainstem glioma

Oren J. Becher[1,3,5], **Dolores Hambardzumyan**[2,5], **Talia R. Walker**[1,5], **Karim Helmy**[1,5], **Javad Nazarian**[6], **Steffen Albrecht**[7], **Rebecca L. Hiner**[3,5], **Sarah Gall**[8], **Jason T. Huse**[1,4,5], **Nada Jabado**[7], **Tobey J. MacDonald**[6], and **Eric C. Holland**[1,2,5]

[1]Cancer Biology and Genetics, MSKCC, New York, NY 10021

[2]Neurosurgery, MSKCC, New York, NY 10021

[3]Pediatrics, MSKCC, New York, NY 10021

[4]Pathology, MSKCC, New York, NY 10021

[5]Brain Tumor Center, MSKCC, New York, NY 10021

[6]Children's National Medical Center Washington, DC 20010

[7]Montréal Children's Hospital, Montréal, Quebec, Canada

[8]Carolinas Medical Center 1001 Blythe Boulevard Charlotte, NC 28203

Abstract

Brainstem gliomas (BSGs) are a rare group of CNS tumors that arise mostly in children and usually portend a particularly poor prognosis. We report the development of a genetically engineered mouse model of BSG using the RCAS/tv-a system and its implementation in preclinical trials. Using immunohistochemistry we found that PDGFRα is overexpressed in 67% of pediatric BSGs. Based on this observation, we induced low-grade BSGs by overexpressing PDGF-B in the posterior fossa of neonatal Nestin tv-a mice. To generate high-grade BSGs, we overexpressed PDGF-B in combination with Ink4a-ARF loss, given that this locus is commonly lost in high-grade pediatric BSGs. We show that the likely cells-of-origin for these mouse BSGs exist on the floor of the 4th ventricle and cerebral aqueduct. Irradiation of these high-grade BSGs shows that while 2, 6, and 10 Gy single doses significantly increased the percent of TUNEL-positive nuclei, only 6, and 10 Gy significantly induces cell-cycle arrest. Perifosine, an inhibitor of AKT signaling significantly induced TUNEL-positive nuclei in this high-grade BSG model, but in combination with 10 Gy, it did not significantly increase the percent of TUNEL-positive nuclei relative to 10 Gy alone at 6, 24, and 72 hours. Survival analysis demonstrated that a single dose of 10 Gy significantly prolonged survival by 27% (p=0.0002) but perifosine did not (p=0.92). Perifosine + 10Gy did not result in a significantly increased survival relative to 10Gy alone (p=0.23). This PDGF-induced BSG model can serve as a preclinical tool for the testing of novel agents.

Keywords

Brainstem glioma; DIPG; perifosine; radiation

Contact Info: Eric C. Holland, Z1304, 408 East 69th Street, New York, NY 10021. Fax: (646) 422-0231; hollande@mskcc.org.

Introduction

Gliomas may arise anywhere in the central nervous system (CNS). An uncommon location for gliomagenesis in the CNS is the brainstem. Brainstem gliomas (BSGs) develop predominantly in the pediatric population where they constitute up to 20% of childhood brain tumors and are the leading cause of death for children with brain tumors (1). According to histopathological characteristics, BSGs are divided into high-grade (WHO Grades III and IV) which comprise about 85% of BSGs (also called DIPGs for diffuse intrinsic pontine gliomas if the tumor is primarily localized to the pons), with the remaining being low-grade (WHO Grades I and II). By contrast, BSGs in adults are much less common, accounting for <2% of gliomas. Furthermore, brainstem gliomas in adults are less aggressive than those in children and are thought to be biologically different (2).

Focal radiation consisting of daily 2 Gy doses for approximately 30 doses over six weeks is the current standard of care for these tumors - a treatment modality that unfortunately provides only temporary relief of symptoms. Despite numerous clinical investigations to date there have been no chemotherapeutic or biological agents that have proven clearly beneficial for the treatment of high grade BSGs in children. The median survival for these children is less than 1 year after diagnosis, although it has been observed that children less than 3 years of age may fare better (3).

There is limited understanding of the biology of BSGs in children due to limited availability of clinical specimens. As these tumors are not routinely resected and autopsy rates are quite low, such clinical specimens are extremely precious (4). The limited studies published on this entity demonstrate that these tumors have similar genetic alterations as pediatric gliomas arising in other parts of the brain, but distinct from the molecular characteristics of adult gliomas (5-10). ERBB1 is amplified in a small subset of brainstem gliomas and overexpressed in a larger subset (11). Kras and AKT activation have been described in 60% of pediatric high-grade gliomas including several brainstem gliomas (12). P53 mutations have been described ranging from 29-71% of pediatric brainstem gliomas (8, 10, 13-16). The most common reported molecular alterations occur in PDGFR, which is overexpressed in about 30%-80% of high-grade gliomas including brainstem gliomas (17-19), and loss of expression of Ink4a-ARF, which has been described ranging from 17-100% of pediatric glioblastomas in the brainstem (8,16,20).

There are two published rat models of BSG, both are allograft models using cell-lines derived from rat cortical gliomas that are stereotactically implanted into the brainstem. The rats develop tumors in the brainstem but it is not clear to what extent these accurately model the histology and genetics of the human disease (21,22). The cell-lines are derived from a carcinogen-induced cortical glioma, and are maintained in serum-conditions prior to implantation, culture conditions that has been shown to be inferior to culturing in bFGF and EGF in maintaining the phenotype and genotype of primary gliomas (23). In addition, a human xenograft brainstem glioma model in rats has also been recently reported which uses adult glioma cell-lines that arose from adult cortical gliomas and are implanted into immunodeficient rats (24). To our knowledge there is no genetically engineered mouse model for this disease.

Here we initially observed that PDGFRα is overexpressed in 67% of high-grade BSGs overall, including 87% of biopsy specimens. We utilized the RCAS/tv-a system to overexpress PDGF-B in nestin expressing cells lining the 4th ventricle and aqueduct. This gene transfer resulted in the formation of low-grade BSGs, while PDGF overexpression in conjunction with Ink4a-ARF loss in the same periventricular cells resulted in the formation of high-grade BSGs. These tumors were histologically similar to diffuse pediatric BSGs in

many respects. A short-term analysis of RT in this BSG model showed that higher doses of RT are more effective in inducing cell cycle arrest. As the AKT pathway is thought to mediate radioresistance (25), we tested perifosine, an inhibitor of AKT signaling, alone and in combination with RT in this BSG model. Perifosine treatment significantly increased TUNEL-positive nuclei, but in combination with RT, perifosine did not significantly increase TUNEL-positive nuclei relative to RT alone at 6, 24, or 72 hours post RT. Survival analysis demonstrated that single dose 10Gy increased survival of high-grade BSG-bearing mice by 27% (57days vs. 45days; p=0.0002) while perifosine monotherapy did not. Pretreatment of 10Gy RT with perifosine did not result in a significantly increased median survival relative to 10Gy alone (64 days vs. 57 days p=0.23). In summary, our PDGF-induced BSG model is the first genetically engineered BSG mouse model that may serve as useful preclinical model for testing of novel treatment regimens.

Materials and Methods

Generation of BSGs

To generate BSGs, we injected 1μl (10^5cells) of RCAS-PDGFB expressing DF1 cells into Ntv-a or Ntv-a; Ink4a-ARF −/− mice. The genetic background of our Ntv-a mice is a mix of BALB/c, FVB, B6, 129 and SW strains. INK4a-ARF −/−; Ntv-a strain is a mix of BALB/c, FVB, B6, and 129 strains. Greater than 20 generations of backcrossing was done to generate the lines. Injections were intracranial, 2mm posterior to the bregma at the midline position within 72 hours of birth using a Hamilton syringe. Mice were monitored carefully for signs of tumor development (hydrocephalus, lethargy, head tilt). Upon the appearance of brain tumor symptoms, mice were euthanized with CO_2, brain tissue extracted, fixed in formalin, and paraffin embedded.

Investigation of the cell of origin of BSGs

To determine the cell of origin, we injected 1μl (10^5cells) of DF1 cells expressing RCAS-GFP or RCAS-RFP into Ntv-a mice as described above. Mice were euthanized 24 hours later (n=2) or at four weeks of age (n=6). Their brain tissue was then extracted, postfixed for 30 minutes in 4% PFA, transferred into 30% sucrose at 4°C for cryoprotection, embedded in OCT, frozen on dry ice, and stored at −80°C. Brains were sectioned in 10μm sections and inspected with fluorescent microscope for GFP or RFP labeled cells.

Treatment of BSG bearing mice

We used total-body irradiation (TBI) for all the irradiation experiments with the exception of the survival analysis. TBI was delivered with a Gamma Cell 40 Irradiator (MDS Nordion) that delivers 106cGy/min. For survival analysis, mice were sedated with ketamine and xylazine, and irradiation of the head was done using a X-RAD 320 from Precision X-Ray at 115 cGy/min (the rest of the mouse was shielded with a lead jig). Perifosine treatment was IP at a dose 30mg/kg/day (in normal saline) once daily and was for a minimum of three daily doses. Combination perifosine and RT was done as follows: perifosine given daily for 3 days as monotherapy, followed by single dose RT. At the end of the treatment, mice were euthanized, brains were dissected, and placed in formalin.

Immunohistochemistry

Immunohistochemistry on mouse and human FFPE sections was performed using Discovery XT (Ventana Medical Systems, Tucson, AZ). Human BSG tissue was obtained from MSKCC, CNMC, Montreal Children's Hospital, and Carolinas Heathcare System. Analysis of human BSG tissue was IRB approved at all institutions. The following antibodies were used: PDGFRα (Cell Signaling, #3164 1:100), Ki-67 (DAKO 1:100 Human; Vector for

Mouse), PhosphoH3-Ser10 (Upstate 1:800), Olig2- (Millipore; 1:250), GFAP (DAKO 1:1000). For immunofluorescence, we used anti-RFP antibody from Rockland at 1:200 followed by Alexxa 488 anti-Rabbit secondary antibody both as per manufacturer's protocol. The TUNEL assay was performed per Roche's instructions (#3333566).

Quantitative Analysis

All immunohistochemistry slides were scanned. One observer (OJB) performed the quantification of TUNEL, pH3, and Ki-67 using the program Metamorph where a threshold was set for TUNEL, pH3 and Ki67 and applied to all sections analyzed. At least 5 high-magnification 20× representative areas were analyzed per tumor. For quantification of pH3, positive cells were at least 5 pixels of positive area. For quantification of TUNEL-positive nuclei, we excluded pseudopalisades.

MRI

MRI of murine gliomas has been previously described (26).

Results

PDGFRα is overexpressed in Pediatric high-grade BSGs

To specifically investigate the PDGFRα expression in pediatric high-grade BSGs biopsy and autopsy specimens, we immunostained paraffin sections of high-grade BSGs for PDGFRα and noted that twelve out of eighteen (67%) of high-grade BSGs contained tumor cells that express PDGFRα (Table 1). Interestingly, we noted that seven out of eight surgical biopsies of BSGs had PDGFRα overexpression (87.5%), while only five out of ten autopsies expressed PDGFRα (50%). The difference in expression of PDGFRα between surgical biopsies and autopsies was not statistically significant (Two tail fisher's exact test p=0.15).

Generation of PDGF-induced brainstem gliomas in mice

PDGFRα overexpression is a common event in pediatric high-grade BSGs, and so we were interested to determine if overexpression of PDGF in the posterior fossa of neonatal Ntv-a mice can induce brainstem gliomas. We infected RCAS-PDGF into the posterior fossa of Ntv-a neonatal mice within 72 hours of birth (approximately 2mm posterior and midline to the bregma), and observed the mice for signs and symptoms of brain tumor formation. PDGF overexpression in Ntv-a mice resulted in low-grade BSGs (Grade II; Figure 1B). The incidence of tumor formation was 80% (12 out of 15) and most of the mice were asymptomatic until euthanasia at 12 weeks (Figure 1A). Of note, no embryonal tumors (such as medulloblastomas) were observed, and the cerebellar external granule layer was not altered.

The tumor cells of these low-grade gliomas were proliferating at a low rate with a Mib1 index of 0.83± 0.16%. There was minimal baseline apoptosis as observed with cleaved caspase 3 immunohistochemistry (data not shown). The low-grade gliomas were not purely astrocytic as most of the cells in these lesions immunostained for Olig-2. These lesions were not simply reactive gliosis as they were quite large at 12 weeks with several tumors occupying approximately 50% of the pons. These lesions were easily visible on MRI (Figure1B). Mice injected with vector alone did not show any lesions. The single mouse that died developed obstructive hydrocephalus due to tumor. Characteristic immunostains of these lesions are illustrated in Figure 2C (Ki-67, Olig-2, PDGFR), and can be contrasted with immunostains of normal brainstem (Figure2D). In addition there is a GFAP immunostain of a low-grade BSG in Supplemental Figure 1A.

High-grade BSGs in humans show *Ink4a-ARF* loss, and therefore, we added this genetic alteration to our model. Ntv-a mice with deletion of *Ink4a-ARF* infected with RCAS-PDGF developed symptoms of brain tumor formation such as macrocephaly, lethargy, and hemiparesis between four and eight weeks. We sacrificed these symptomatic animals and extracted their brains. All of the mice had grade IV BSGs with pathological elements of microvascular proliferation and pseudopalisading necrosis (Figure 1C). The incidence and latency for PDGF overexpression in Ink4a/Arf null mice was 96% (68 out of 71) with a median survival of 31.5 days (Figure 1A). The survival of mice with high-grade BSGs induced in *Ink4a-ARF*−/− background was significantly shorter than that of mice with low-grade BSGs ($p<0.0001$ using log-rank test). We obtained an MRI of a subset of symptomatic mice prior to sacrificing the animals and could easily visualize the brainstem tumors in all cases (Figure 1C). We examined the brainstems of at least fifty uninjected Ntv-a mice with deletion of *Ink4a-ARF* and did not observe any preneoplastic lesions.

The anatomical extent of the tumors at 4 weeks was that 80% of the tumors localized completely within the brainstem (based on T2 weighted MRI images). The natural course of these tumors based on serial MRIs was that the tumors would go on to invade into the cerebellum posteriorly and invade anteriorly and superiorly into the thalamus and top of the brainstem respectively. Eventually all the mice developed obstructive hydrocephalus that likely resulted in obstruction of the CSF flow at the level of the 4th ventricle and aqueduct and its associated symptoms. Mice were euthanized at that point. The tumor volume estimate at 4 weeks (measurements were done on T2 weighted MRI images of at least 10 high-grade BSGs) was 11.9mm^3 +/−4.7mm^3. Histological examination revealed that 70% of the tumors occupied at least 50% of the pons.

The histological appearance of our murine BSGs was similar to human pediatric BSGs, particularly with regard to the diffusely infiltrating arrangement of the tumor cells (Figure 2A and 2B). We immunostained our murine BSGs for Ki-67, Olig 2, GFAP, and PDGFRα, and we noted further similarities between these tumors and pediatric BSGs. Pediatric BSGs stained positive for Olig-2 but with large variability in the percent of positive cells in different tumors ranging from 10% to nearly 100%, while greater than 90% of the tumor cells of our PDGF induced BSGs in Ink4a-ARF−/− mice stained strongly for PDGFRα and for Olig-2 (Figure 2A,B and Supplemental Figure 2). GFAP immunostaining was positive in both low and high-grade murine BSGs, with similarity to pediatric BSGs (Supplemental Figure 1,2). Of note, Mib-1 labeling was 10.2± 5.6% for PDGF-induced BSGs in Ink4a-ARF−/− background.

RCAS infections target cells on the ventricular surface of the 4th ventricle

The RCAS/tv-a system allows for lineage tracing of tv-a expressing cells infected with RCAS. As we were using the Ntv-a mouse, we were infecting only nestin-expressing cells. Nestin expression in the ependymal layer of the 4th ventricle has been previously described before in humans (27). In addition, it has been hypothesized that cells lining the floor of the fourth ventricle may serve as cells-of-origin for brainstem gliomas (28). We therefore decided to investigate which cells we were targeting with our infections (29,30).

We injected DF-1 cells producing RCAS-RFP into the posterior fossa of neonatal Ntv-a mice at P2 (n=2). 24 hours later we euthanized both neonatal mice, extracted their brains, sectioned and looked for RFP labeled cells. Both mice had RFP labeled cells floating in the cerebrospinal fluid and were localized around the 4th ventricle and aqueduct (Supplemental Figure 3). In parallel, we injected DF-1 cells producing RCAS-GFP in a similar fashion at P2 (n=6). We monitored the mice for four weeks (DF-1 cells have been previously reported to survive up to three weeks after injection), euthanized the mice, extracted their brains, and looked for GFP labeled cells. The cells expressing GFP were located mostly in the outer

layer of the 4th ventricle (Figure 3A) or aqueduct. Of note, the distribution was not random, (Figure 3B). We found that more than 90% of the GFP labeled cells were located symmetrically at specific locations on the ventricular surface of the floor of the 4th ventricle, while only 5% were from the roof of the fourth ventricle (266 GFP labeled cells counted). In addition, we immunostained sections of neonatal pups at postnatal days 1-3 and noted strong nestin expression in the cells lining the 4th ventricle during this early postnatal age (both roof and floor of fourth ventricle as seen in Figure 3C).

To confirm that the nestin-expressing cells of the 4th ventricle and aqueduct are the cells- of-origin for our murine BSG model, we infected RCAS-PDGF as described above, observed the mice for three weeks, euthanized them, and looked for neoplastic lesions. We noted that all of the mice had small precursor lesions and 80% of the precursor lesions (12 out 15) were arising from the floor of the 4th ventricle or aqueduct (Figure 3D).

In summary, we have developed a genetically engineered BSG model that has histological similarities to human BSGs and has comparable immunostaining characteristics. Our BSG model arises from the cells of the 4th ventricle or aqueduct. Next we were interested to use this BSG model in preclinical trials

Preclinical trials on the mouse BSG model

RT is the only known therapeutic modality with antitumor activity for children with BSGs. Therefore, we investigated this treatment in our mouse model. We irradiated PDGF-induced high-grade BSG-bearing mice with single dose RT at 2 Gy (approximately the dose used in the clinic), 6 Gy, and 10 Gy, and sacrificed the mice at three time-points: 6 hours, 24 hours, and 72 hours (minimum 5 mice per group). We analyzed the response of these tumors to irradiation using TUNEL and evaluated the proliferation rate using phosphoH3 (pH3). 10 Gy and 6 Gy induced a near complete cell-cycle arrest six hours post treatment as evaluated by pH3, but 2 Gy did not significantly affect pH3 (Figure 4A and B). We also found significantly increased TUNEL-positive nuclei, relative to unirradiated BSGs at 24 hours post RT for all doses of RT analyzed (Figure 4 C and D). 10 Gy time-course demonstrated that the peak inhibition of proliferation was 6 hours post RT and that the highest percent of TUNEL-positive nuclei was 24 hours post RT (Supplemental Figure 4A,B). To determine if RT prolongs survival in this BSG model we treated BSG-bearing mice with single dose 10 Gy (by only irradiating the head). Treatment was begun after pretreatment MRIs at four weeks so that similarly sized tumors were assigned to each treatment group (including untreated group). 10 Gy single dose prolonged survival by 12 days (Figure 5D; 57days vs. 45 days; p=0.0002). A 2 Gy single dose did not prolong survival significantly (p=0.14). In summary, high-dose RT is effective in prolonging survival in this BSG model.

Combination of Perifosine and RT in this high grade BSG model

We recently noted that perifosine, an inhibitor of AKT signaling, cooperates with radiation in medulloblastomas (31). In addition, the AKT pathway has been demonstrated to be active in radioresistant glioma cells, and we have previously shown that perifosine cooperates with temozolomide in gliomas (25,32). Therefore, we determined whether perifosine has a therapeutic effect in brainstem gliomas as a single agent and in combination with 10 Gy RT, the most effective single radiation dose. We treated a group of PDGF-induced high-grade BSGs with perifosine alone for 3-5 days, as well as a second group with three days of perifosine followed by single dose 10 Gy. Perifosine treatment did not affect proliferation significantly as a single agent and there was no statistically significant difference in proliferation with the addition of perifosine to 10Gy RT at 6, 24 and 72 hours as measured with pH3 (Mann-Whitney p=0.7, p=0.28, and p=0.06 respectively, Figure 5A). The percent of TUNEL-positive nuclei increased significantly with treatment with perifosine (Mann-

Whitney p=0.005), but the combination of perifosine+ 10 Gy did not significantly affect the percent of TUNEL-positive nuclei relative to 10 Gy alone at 6, 24, and 72 hrs post RT (Mann-Whitney p=0.46, p=0.15, and p=0.09 respectively; Figure 5B). To investigate the long-term effect of these treatments, survival analysis was carried out to determine if perifosine will prolong survival as monotherapy or in combination with RT (using head irradiation) in this high-grade BSG model. Single agent daily perifosine treatment for one week did not prolong survival (43 days vs. 45 days; p=0.92), and pre-treatment with perifosine prior to 10Gy RT did not result in a significantly increased survival relative to 10Gy RT alone (64 days vs. 57 days; p=0.23; Figure 5C, 5D). Our results suggest that perifosine, when used a single agent or with single dose 10Gy, does not have sufficient antitumor activity to prolong survival in this model.

Discussion

In this study we applied RCAS/tv-a technology to generate brainstem gliomas that can be used for preclinical trials. There are numerous advantages to this preclinical model. First, it is consistent with the genetic alterations of a subset of the human disease according to the published literature and our analysis of human specimens. Second, It is histologically similar to the human disease. Third, the tumors arise in immunocompetent mice. Fourth, the model has high penetrance and short latency, and forms in the appropriate microenvironment- the brainstem. Fifth, this model responds to, but is not cured with RT, like the clinical experience of treating children with DIPGs with focal RT. Sixth, the pattern of invasion of the PDGF-induced high-grade BSGs is similar to the pattern of invasion of human high-grade BSGs as a subset of the latter have been described to contiguously involve the cerebellar peduncles, cerebellum, and/or thalamus (33). It thus may serve as a preclinical model for screening of novel agents. There are only a few hundred new cases of pediatric BSGs in the world each year, and as there are now an increasingly large number of novel agents and exponential combinations of these agents- a genetic mouse model may be useful to screen for the most active combinations and schedules.

The cell-of-origin for supratentorial NF-1 deleted gliomas have been proposed to be neural stem cells from the subventricular zone (34). However, other modeling systems indicate that nestin expressing cells in other areas of the brain are also able to serve as the cell of origin (26). Here we present evidence that the cells-of-origin for this murine brainstem glioma model are mostly localized to the surface of the 4th ventricle and aqueduct. Other cells in the brainstem may also serve as the cells-of-origin for the development of murine BSGs but as we used the Ntv-a mouse, we restricted our investigation to nestin expressing cells in the brainstem in the neonatal period – which are the cells lining the 4th ventricle and aqueduct.

We evaluated external beam irradiation in this BSG model and noted that similar to the clinical experience of treating children with DIPGs with focal RT, radiation therapy is active in this model. It is important to note that the results of our preclinical testing with single doses of irradiation do not suggest that higher doses of irradiation will be more beneficial to treat children with DIPGs. A single dose of 10 Gy is a potentially toxic dose to the normal cells in the brainstem and higher total doses of radiation have been tested in clinical trials for DIPGs using hyperfractionated radiation and did not demonstrate increased efficacy (35). As BSGs are heterogeneous tumors, observations with this mouse model may only apply to BSGs that overexpress PDGFR and have lost Ink4a-Arf. If this was the case, pretreatment tissue to determine genetic status would be needed, and obtaining biopsies for DIPGs has recently been reported to have minimal complications (36). However, it is important to note that to biopsy DIPGs is a controversial topic, its success is highly dependent on who performs it, and it is hard to obtain approval for it in clinical trials (37).

We extended the preclinical testing by evaluating perifosine, an inhibitor of AKT signaling, alone and in combination with RT using this model. Our analysis showed that while perifosine monotherapy has modest activity in inducing cell-death in short-term analysis in this model it does not have enough antitumor activity to increase survival. In addition, perifosine did not provide additional survival benefit to high dose RT. This is perhaps not surprising as there is no drug that has been shown to increase survival of children with high-grade BSGs in numerous clinical trials even in combination with RT, and may be due to the poor drug delivery into the brainstem due to the blood brain barrier. This observation reinforces our recommendation that novel combinations should be tested in a genetically and histologically accurate preclinical model first prior to their translation to the clinic.

Supplementary Material

Refer to Web version on PubMed Central for supplementary material.

Acknowledgments

We thank Katia Manova, Sho Fujiwama, Jim Finney, Quancho Zhang, Carl Le, Dov Winkelman, and Mihaela Lupu. OJB is a St. Baldrick's scholar and is supported by MSKCC BTC, MLF and Witmer foundations, K12 Award. ECH is supported by Kirby foundation, R01 CA100688, U01 CA141502, and U54 CA126518.

References

1. Hargrave D, Bartels U, Bouffet E. Diffuse brainstem glioma in children: critical review of clinical trials. Lancet Oncol. 2006; 7:241–8. [PubMed: 16510333]
2. Guillamo JS, Monjour A, Taillandier L, et al. Brainstem gliomas in adults: prognostic factors and classification. Brain. 2001; 124:2528–39. [PubMed: 11701605]
3. Broniscer A, Laningham FH, Sanders RP, Kun LE, Ellison DW, Gajjar A. Young age may predict a better outcome for children with diffuse pontine glioma. Cancer. 2008; 113:566–72. [PubMed: 18484645]
4. Leach PA, Estlin EJ, Coope DJ, Thorne JA, Kamaly-Asl ID. Diffuse brainstem gliomas in children: should we or shouldn't we biopsy? Br J Neurosurg. 2008; 22:619–24. [PubMed: 19016112]
5. Puputti M, Tynninen O, Sihto H, et al. Amplification of KIT, PDGFRA, VEGFR2, and EGFR in gliomas. Mol Cancer Res. 2006; 4:927–34. [PubMed: 17189383]
6. Di Sapio A, Morra I, Pradotto L, Guido M, Schiffer D, Mauro A. Molecular genetic changes in a series of neuroepithelial tumors of childhood. J Neurooncol. 2002; 59:117–22. [PubMed: 12241104]
7. Wong KK, Tsang YT, Chang YM, et al. Genome-wide allelic imbalance analysis of pediatric gliomas by single nucleotide polymorphic allele array. Cancer Res. 2006; 66:11172–8. [PubMed: 17145861]
8. Sung T, Miller DC, Hayes RL, Alonso M, Yee H, Newcomb EW. Preferential inactivation of the p53 tumor suppressor pathway and lack of EGFR amplification distinguish de novo high grade pediatric astrocytomas from de novo adult astrocytomas. Brain Pathol. 2000; 10:249–59. [PubMed: 10764044]
9. Liang ML, Ma J, Ho M, et al. Tyrosine kinase expression in pediatric high grade astrocytoma. J Neurooncol. 2008; 87:247–53. [PubMed: 18193393]
10. Cheng Y, Ng HK, Zhang SF, et al. Genetic alterations in pediatric high-grade astrocytomas. Hum Pathol. 1999; 30:1284–90. [PubMed: 10571506]
11. Gilbertson RJ, Hill DA, Hernan R, et al. ERBB1 is amplified and overexpressed in high-grade diffusely infiltrative pediatric brain stem glioma. Clin Cancer Res. 2003; 9:3620–4. [PubMed: 14506149]
12. Faury D, Nantel A, Dunn SE, et al. Molecular profiling identifies prognostic subgroups of pediatric glioblastoma and shows increased YB-1 expression in tumors. J Clin Oncol. 2007; 25:1196–208. [PubMed: 17401009]

13. Badhe PB, Chauhan PP, Mehta NK. Brainstem gliomas—a clinicopathological study of 45 cases with p53 immunohistochemistry. Indian J Cancer. 2004; 41:170–4. [PubMed: 15659871]
14. Louis DN, Rubio MP, Correa KM, Gusella JF, von Deimling A. Molecular genetics of pediatric brain stem gliomasc Application of PCR techniques to small and archival brain tumor specimens. J Neuropathol Exp Neurol. 1993; 52:507–15. [PubMed: 8103086]
15. Zhang S, Feng X, Koga H, Ichikawa T, Abe S, Kumanishi T. p53 gene mutations in pontine gliomas of juvenile onset. Biochem Biophys Res Commun. 1993; 196:851–7. [PubMed: 8240361]
16. Sure U, Ruedi D, Tachibana O, et al. Determination of p53 mutations, EGFR overexpression, and loss of p16 expression in pediatric glioblastomas. J Neuropathol Exp Neurol. 1997; 56:782–9. [PubMed: 9210874]
17. Thorarinsdottir HK, Santi M, McCarter R, et al. Protein expression of platelet- derived growth factor receptor correlates with malignant histology and PTEN with survival in childhood gliomas. Clin Cancer Res. 2008; 14:3386–94. [PubMed: 18519768]
18. Nakamura M, Shimada K, Ishida E, et al. Molecular pathogenesis of pediatric astrocytic tumors. Neuro Oncol. 2007; 9:113–23. [PubMed: 17327574]
19. Geoerger B, Morland B, Ndiaye A, et al. Target-driven exploratory study of imatinib mesylate in children with solid malignancies by the Innovative Therapies for Children with Cancer (ITCC) European Consortium. Eur J Cancer. 2009; 45:2236–8. [PubMed: 19540747]
20. Wakabayashi T, Natsume A, Hatano H, et al. p16 promoter methylation in the serum as a basis for the molecular diagnosis of gliomas. Neurosurgery. 2009; 64:455–61. [PubMed: 19240607]
21. Jallo GI, Volkov A, Wong C, Carson BS Sr, Penno MB. A novel brainstem tumor model: functional and histopathological characterization. Childs Nerv Syst. 2006; 22:1519–25. [PubMed: 17021732]
22. Liu Q, Liu R, Kashyap MV, et al. Brainstem glioma progression in juvenile and adult rats. J Neurosurg. 2008; 109:849–55. [PubMed: 18976074]
23. Lee J, Kotliarova S, Kotliarov Y, et al. Tumor stem cells derived from glioblastomas cultured in bFGF and EGF more closely mirror the phenotype and genotype of primary tumors than do serum-cultured cell lines. Cancer Cell. 2006; 9:391–403. [PubMed: 16697959]
24. Hashizume R, Ozawa T, Dinca EB, et al. A human brainstem glioma xenograft model enabled for bioluminescence imaging. J Neurooncol. 2009
25. Eyler CE, Foo WC, LaFiura KM, McLendon RE, Hjelmeland AB, Rich JN. Brain cancer stem cells display preferential sensitivity to Akt inhibition. Stem Cells. 2008; 26:3027–36. [PubMed: 18802038]
26. Hambardzumyan D, Amankulor NM, Helmy KY, Becher OJ, Holland EC. Modeling Adult Gliomas Using RCAS/t-va Technology. Transl Oncol. 2009; 2:89–95. [PubMed: 19412424]
27. Takano T, Rutka JT, Becker LE. Overexpression of nestin and vimentin in ependymal cells in hydrocephalus. Acta Neuropathol. 1996; 92:90–7. [PubMed: 8811130]
28. Freeman CR, Farmer JP. Pediatric brain stem gliomas: a review. Int J Radiat Oncol Biol Phys. 1998; 40:265–71. [PubMed: 9457808]
29. Holland EC, Celestino J, Dai C, Schaefer L, Sawaya RE, Fuller GN. Combined activation of Ras and Akt in neural progenitors induces glioblastoma formation in mice. Nat Genet. 2000; 25:55–7. [PubMed: 10802656]
30. Dai C, Celestino JC, Okada Y, Louis DN, Fuller GN, Holland EC. PDGF autocrine stimulation dedifferentiates cultured astrocytes and induces oligodendrogliomas and oligoastrocytomas from neural progenitors and astrocytes in vivo. Genes Dev. 2001; 15:1913–25. [PubMed: 11485986]
31. Hambardzumyan D, Becher OJ, Rosenblum MK, Pandolfi PP, Manova-Todorova K, Holland EC. PI3K pathway regulates survival of cancer stem cells residing in the perivascular niche following radiation in medulloblastoma in vivo. Genes Dev. 2008; 22:436–48. [PubMed: 18281460]
32. Momota H, Nerio E, Holland EC. Perifosine inhibits multiple signaling pathways in glial progenitors and cooperates with temozolomide to arrest cell proliferation in gliomas in vivo. Cancer Res. 2005; 65:7429–35. [PubMed: 16103096]
33. Yoshimura J, Onda K, Tanaka R, Takahashi H. Clinicopathological study of diffuse type brainstem gliomas: analysis of 40 autopsy cases. Neurol Med Chir. 2003; 43:375–82.

34. Alcantara Llaguno S, Chen J, Kwon CH, et al. Malignant astrocytomas originate from neural stem/progenitor cells in a somatic tumor suppressor mouse model. Cancer Cell. 2009; 15:45–56. [PubMed: 19111880]

35. Mandell LR, Kadota R, Freeman C, et al. There is no role for hyperfractionated radiotherapy in the management of children with newly diagnosed diffuse intrinsic brainstem tumors: results of a Pediatric Oncology Group phase III trial comparing conventional vs hyperfractionated radiotherapy. Int J Radiat Oncol Biol Phys. 1999; 43:959–64. [PubMed: 10192340]

36. Roujeau T, Machado G, Garnett MR, et al. Stereotactic biopsy of diffuse pontine lesions in children. J Neurosurg. 2007; 107:1–4. [PubMed: 17647306]

37. Albright AL, Packer RJ, Zimmerman R, Rorke LB, Boyett J, Hammond GD. Magnetic resonance scans should replace biopsies for the diagnosis of diffuse brain stem gliomas: a report from the Children's Cancer Group. Neurosurgery. 1993; 33:1026–9. [PubMed: 8133987]

Abbreviations

BSG	brainstem glioma
MRI	magnetic resonance imaging
IHC	immunohistochemistry
RT	radiation therapy

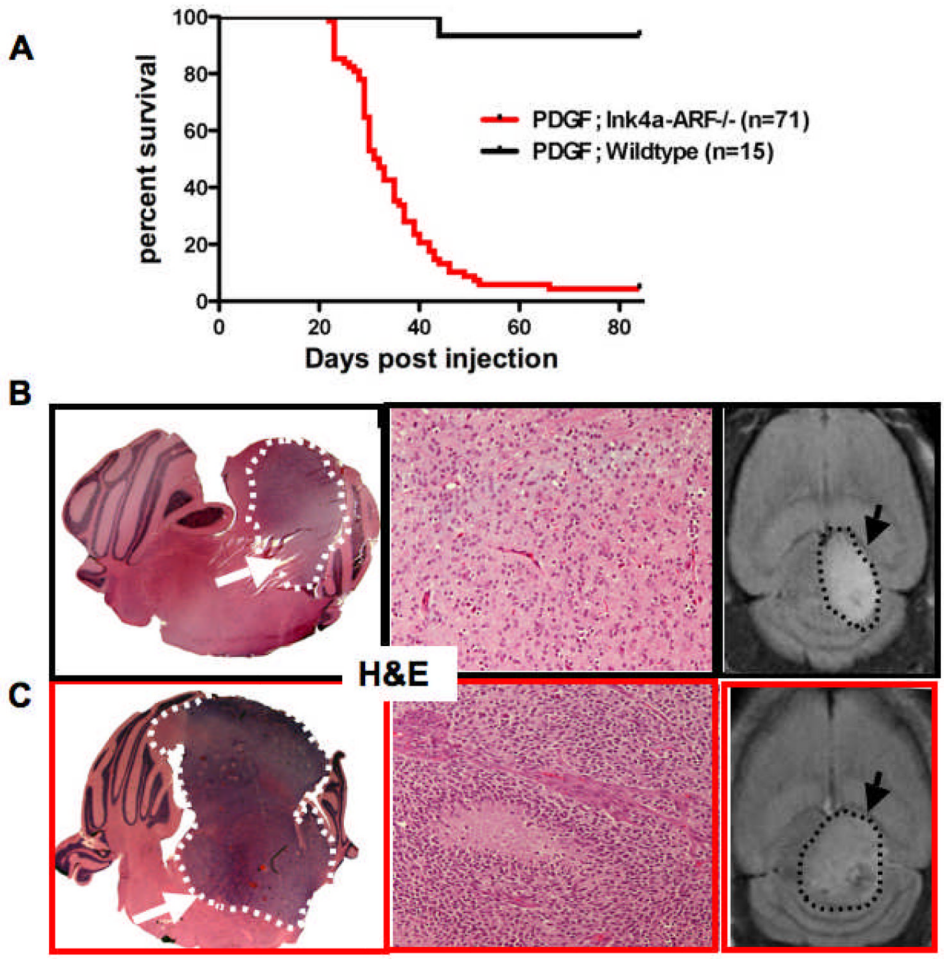

Figure 1. Generation of PDGF-induced Brainstem gliomas

A. Kaplan-Meier of 15 Ntv-a mice, and 71 Ntv-a; Ink4a-ARF−/− mice injected with RCAS-PDGFB. **B**. Low (left) and high (middle) magnification H&E of a PDGF-induced BSG in Ntv-a mouse (sacrificed at twelve-weeks of age). **Right**. T2 weighted image at twelve-weeks of age of a BSG induced by overexpression of PDGF in Ntv-a mouse. **C**. Low (left) and high (middle) magnification H&E of a PDGF-induced BSG in Ntv-a; Ink4a-ARF−/− mouse (sacrificed at five-weeks of age). Right T2 weighted image at four-weeks of age of a BSG induced by overexpression of PDGF in Ntv-a; Ink4a-Arf null mice.

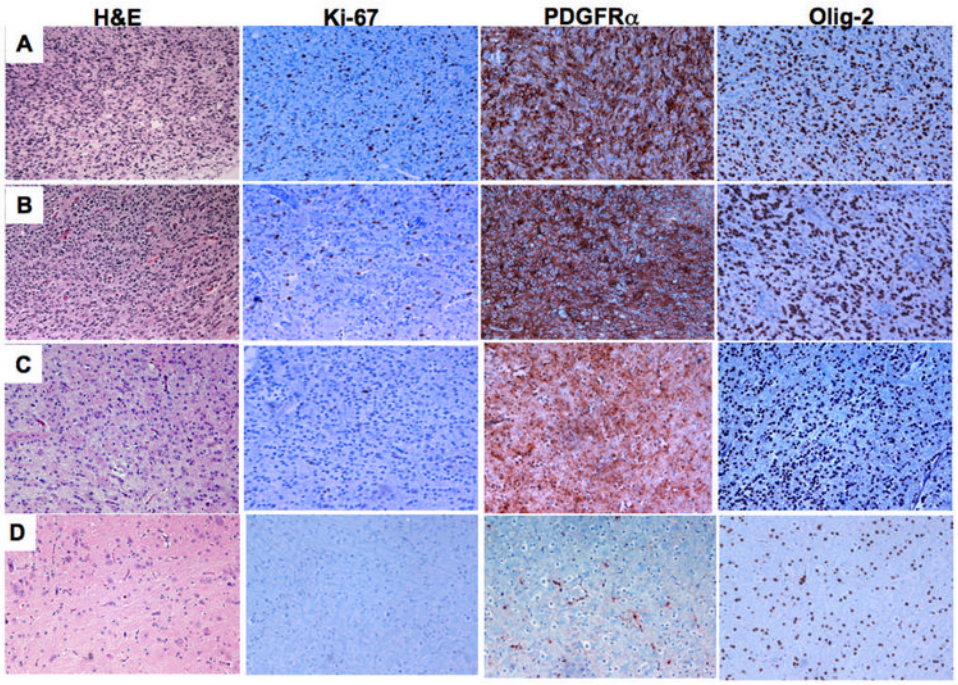

Figure 2. PDGF-induced murine BSGs are histopathologically similar to human BSGs

A. H&E, Ki-67, PDGFRα, and Olig-2 of a pediatric high-grade BSG (human). **B**. H&E, Ki-67, PDGFRα, and Olig-2 of PDGF-induced BSG generated in an Ntv-a; Ink4a-ARF−/− mouse (high-grade BSG). **C**. H&E, Ki−67, PDGFRα, and Olig-2 of PDGF-induced BSG generated in an Ntv-a mouse (low-grade BSG). **D**. H&E, Ki-67, PDGFRα, and Olig-2 of normal brainstem of an Ntv-a; Ink4a-ARF−/− mouse.

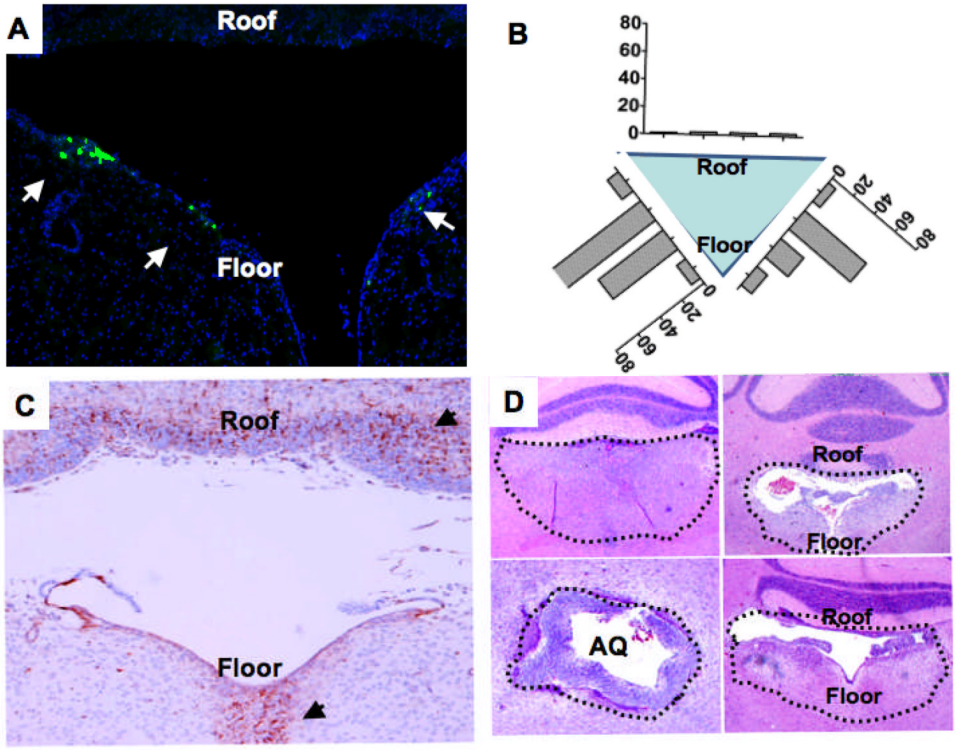

Figure 3. Cell of Origin for murine Brainstem Gliomas

A. High magnification of a cross section from a four-week old Ntv-a mouse infected with RCAS-GFP. White arrows points to clusters of GFP labeled cells. **B**. Quantification of the number of GFP-labeled cells at particular locations of a schematic of the cross section of the 4th ventricle. Y-axis denotes the number of GFP-positive cells and the Y-axis denotes to the location of the GFP-positive cells. This cartoon illustrates the cross-section of the 4th ventricle as a triangle. Each side of the triangle (where the floor of the 4th comprises two sides of the triangle) was divided into 4 equal areas and the number of GFP labeled cells were counted in each area, and tabulated. **C**. High magnification of a cross-section through the 4th ventricle at P2 immunostained with nestin. Black arrows point to positive immunostaining. **D**. Examples of precursor lesions arising from the 4th ventricle or aqueduct of Ntv-a mice infected with RCAS-PDGF (Bottom left is cross section of aqueduct (AQ)).

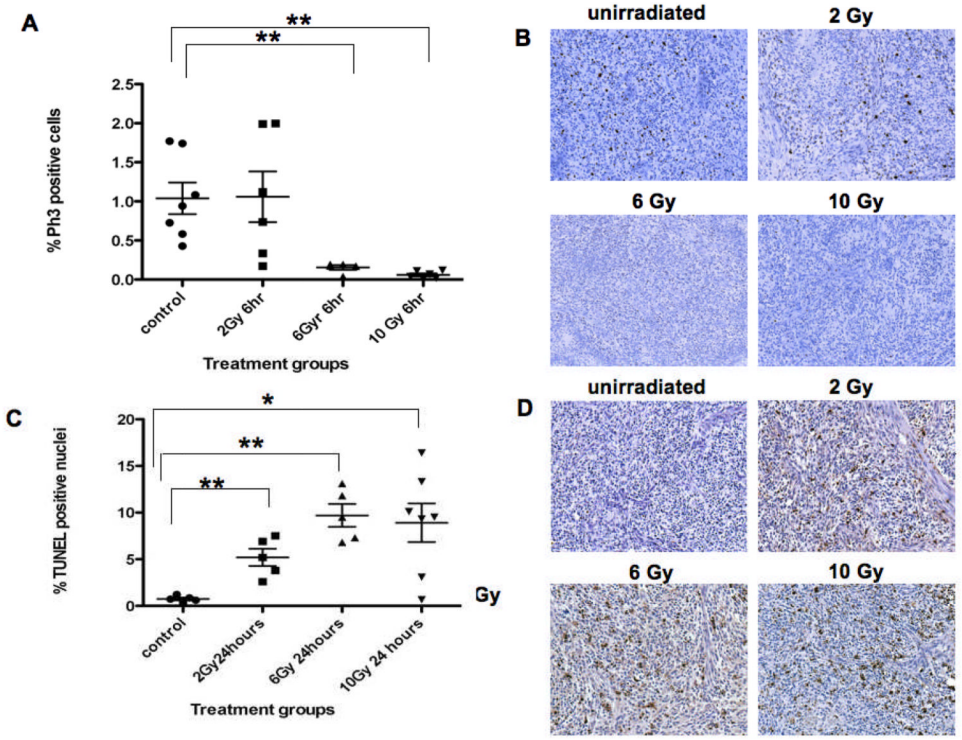

Figure 4. Dose Response Curve for RT of high-grade PDGF-induced BSGs

A. Graph of % pH3 quantification at 6 hours post RT at different doses: 2 Gy (n=6), 6 Gy (n=5), and 10 Gy (n=6) and unirradiated controls (n=7). Mann-Whitney analysis was significant at p=0.0025 between control group and 6 Gy group and was significant at p=0.0012 between control and 10 Gy. We used the following data more than once: control BSGs and 10Gy 6hrs in figure 4A, 5A, and supplemental Figure 4A. **B**. High magnification sections immunostained with pH3: top left: control, top right: 2 Gy, bottom left: 6 Gy and bottom right: 10 Gy. **C**. Graph of % TUNEL-positive nuclei of 2 Gy (n=5), 6 Gy (n=5), and 10 Gy (n=7) and unirradiated controls (n=5) at 24 hours post RT. Mann Whitney analysis was significant at p=0.008 between control and 2 Gy, p=0.008 between control and 6 Gy, and p=0.0243 between control and 10Gy. We used the following data more than once: control BSGs and 10Gy 24hrs in Figure 4C, 5B, and supplemental Figure 4B. **D**. High magnification TUNEL of 2, 6, 10 Gy 24 hours post RT, and unirradiated control.

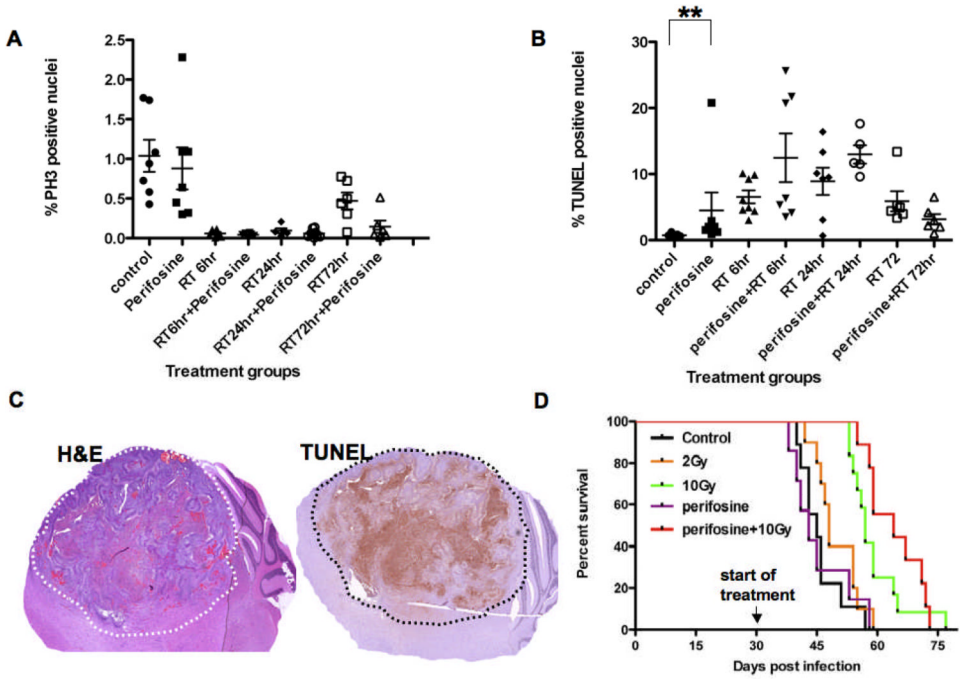

Figure 5. Treatment of PDGF induced Ink4a-ARF null BSGs with Radiation and Perifosine

A. Graph of % pH3 quantification at 6 hours, 24 hours and 72 hours post RT with and without perifosine. Mice per group are denoted in parentheses: untreated (n=7), perifosine (n=7), RT 6hrs (n=6), RT 6hrs + perifosine (n=6), RT 24hrs (n=5), RT 24hrs + perifosine (n=8), RT 72hrs (n=6) and RT 72hrs+perifosine (n=6) **B**. Graph of % TUNEL-positive nuclei at 6 hours, 24 hours, and 72 hours post RT with and without perifosine. Mice per group are denoted in parentheses: untreated (n=5), perifosine (n=7), RT 6hrs (n=8), RT 6hrs + perifosine (n=7), RT 24hrs (n=7), RT 24hrs+ perifosine (n=5), RT 72hrs (n=6), RT 72hrs + perifosine (n=6) **C**. Low magnification H&E (left) and TUNEL(right) of high-grade BSG treated with perifosine+10Gy 6 hours post RT. **D**. Survival analysis of PDGF-induced Ink4a-ARF−/− BSG treated with single dose 2 Gy (10 mice), single dose 10 Gy (12 mice), perifosine (7 mice), perifosine + 10Gy (9 mice), untreated mice (9 mice).

Table 1
Human High-Grade Brainstem Gliomas overexpress PDGFRα

Brainstem Glioma Grade	PDGFR IHC	Biopsy or Autopsy	Age of Patient
Pontine Grade IV	1+	Autopsy	15 year-old
Pontine Grade IV	Negative	Autopsy	4 year-old
Pontine Grade IV	1+	Autopsy	7 year-old
Pontine Grade III	Negative	Autopsy	9 year-old
Pontine Grade IV	Negative	Autopsy	7 year-old
Pontine Grade II	Negative	Autopsy	8 months
Pontine Grade IV	1+ focal	Autopsy	7 year-old
Pontine Grade IV	Negative	Autopsy	10 year-old
Pontine Grade IV	1+ focal	Autopsy	5 year-old
Pontine grade IV	2+	Autopsy	6 year-old
Pontine grade IV	1+	Biopsy	10 year-old
Pontine grade IV	2+	Biopsy	4 year-old
Pontine Grade II	1+	Biopsy	4 year-old
Pontine Grade III	1+	Biopsy	4 year-old
Pontine Grade IV	Negative	Biopsy	8 year-old
Pontine grade IV	2+	Biopsy	4 year-old
Pontine grade IV	2+	Biopsy	10 year-old
Midbrain Grade III	2+	Biopsy	2 year-old

PDGFR IHC (negative = no staining, 1+ = weak staining of tumor cells, and 2+ = strong immunostaining of tumor cells)